Inorganic Chemistry

Article

pubs.acs.org/IC

Hydrothermal Descriptive Chemistry and Single Crystal Structure Determination of Cesium and Rubidium Thorium Fluorides

Christopher C. Underwood, Matthew Mann, Colin D. McMillen, and Joseph W. Kolis*

Department of Chemistry, Clemson University, Clemson, South Carolina 29634-0973, United States

Supporting Information

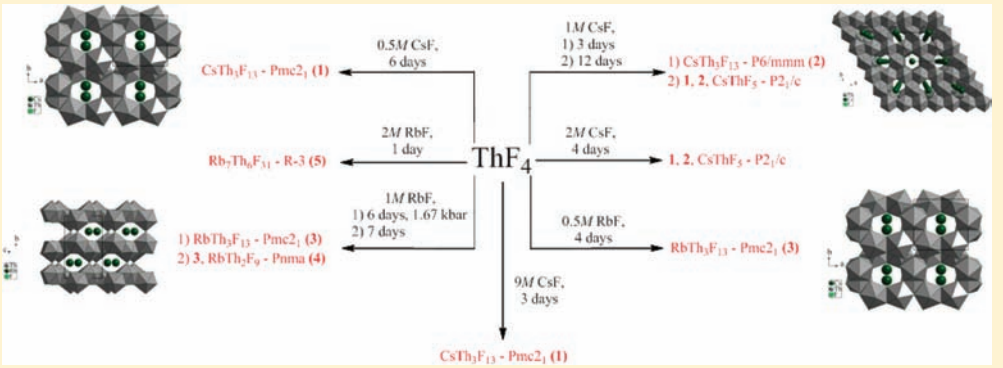

ABSTRACT: Two new cesium thorium fluorides and three new rubidium thorium fluorides have been synthesized hydrothermally and structurally characterized. The structures of two polymorphs of $CsTh_3F_{13}$ are described in space group *P6/mmm* with $a = 8.2608(14)$ and $c = 8.6519(17)$ and space group $Pmc2_1$ with $a = 8.1830(16)$, $b = 7.5780(15)$, and $c = 8.6244(17)$. The analogous orthorhombic compound $RbTh_3F_{13}$, with $a = 8.1805(16)$, $b = 7.4378(15)$, and $c = 8.6594(17)$ in space group $Pmc2_1$, is also reported. Two other rubidium thorium fluorides are also described: $RbTh_2F_9$ crystallizes in the space group *Pnma* where $a = 8.9101(18)$, $b = 11.829(2)$, and $c = 7.4048(15)$, and $Rb_7Th_6F_{31}$ crystallizes in the space group $R\bar{3}$ where $a = 15.609(2)$ and $c = 10.823(2)$. Comparison of these materials was made on the basis of their structures and synthesis conditions. The formation of these species in hydrothermal fluids appears to be dependent upon the concentration of the alkali fluoride mineralizer solution and, thus, the ratio of alkali ions to thorium in the system.

1. INTRODUCTION

The descriptive chemistry of solid-state inorganic thorium compounds received considerable attention in the early era of atomic energy[1] but has been somewhat neglected in the past several decades. However, it may be worthy of new interest because of the possible use of thorium as a safe nuclear fuel in the future. Unlike uranium or plutonium, thorium cannot be weaponized or undergo meltdown in a reactor. The U.S. has enormous amounts of extractable thoria ore on shore, making it an intriguing material for next generation nuclear energy.[2] As such, we feel that the fundamental descriptive chemistry of thorium is worthy of revisiting.

Recently, we found that thorium oxide can be grown as large high-quality single crystals using fluoride mineralizers in hydrothermal fluids.[3] This suggests that further chemistry of inorganic thorium salts under hydrothermal conditions may be fruitful. One class of compounds of particular interest is the alkali thorium fluorides. These compounds are of technological interest because the next generation of both fusion and fission reactors may employ molten alkali thorium fluorides as a fuel source.[2a] Previous work was done primarily in molten alkali fluoride salts and led to a variety of alkali metal thorium fluorides in the tetravalent state. A considerable number of $A_xTh_yF_z$ compounds were characterized, mostly by either powder or single crystal diffraction.[1,4−30] Most of these phases are sodium and potassium thorium fluorides with, to our knowledge, only one rubidium thorium fluoride and no cesium-containing examples previously reported as single crystal structures.

Most of these early results are nearly 40 years old. Given the renewed technological interest in thorium chemistry and the interesting behavior of the oxides in hydrothermal fluids, we undertook a new study of thorium fluorides in hydrothermal fluids. We found that the chemistry of the thorium fluorides is much richer than anticipated. In general, the reaction of ThF_4 with alkali fluorides in hydrothermal fluids leads to a wide variety of new alkali metal thorium fluoride compounds. Systematic exploration of the phase space has uncovered a number of species that typically reflect the size and stoichiometry of the alkali ion. Perhaps surprisingly we rarely observe any hydrolysis of the Th−F bond, even in aqueous solution above 600 °C. Furthermore, inclusion of alkaline earth ions in the solution leads to ready formation of mixed alkali−alkaline earth thorium fluorides,[31] suggesting that much of the phase space is still unexplored. In this paper, we describe the chemistry and

Received: September 6, 2011
Published: October 27, 2011

Table 1. Specific Reaction Conditions for the Syntheses of the Title Solids

condition[a]	mineralizer	alkali/th ratio	pressure(kbar)	time (days)	crystal shape(s)	compound
1	CsF, 9 M	7.4:1	1	3	polyhedra	$CsTh_3F_{13}$ ($Pmc2_1$) (**1**)
2	CsF, 0.5 M	0.41:1	1	6	polyhedra	**1**
3	CsF, 1 M	0.82:1	1	3	hexagonal rods	$CsTh_3F_{13}$ ($P6/mmm$) (**2**)
4	CsF, 2 M	1.6:1	1	4	square rods, polyhedra	**1**, **2**, $CsThF_5$[b]
5	CsF, 1 M	0.82:1	1	12	square rods, polyhedra, hexagonal plates	**1**, **2**, $CsThF_5$[b]
6	RbF, 0.5 M	0.41:1	1	4	polyhedra	$RbTh_3F_{13}$ ($Pmc2_1$) (**3**)
7	RbF, 1 M	0.82:1	1	7	polyhedra	**3**
8	RbF, 1 M	0.82:1	1.67	6	polyhedra, plates	**3**, $RbTh_2F_9$ ($Pnma$) (**4**)
9	RbF, 2 M	1.6:1	1.5	1	polyhedra	$Rb_7Th_6F_{31}$ ($R\bar{3}$) (**5**)
10	RbF, 9 M	7.4:1	1	3	polyhedra	**5**

[a]All condition temperatures are 575 °C. [b]The polymorphism of $CsThF_5$ is quite complex and is the subject of a separate, forthcoming report.

structures of a series of new alkali thorium fluorides grown from hydrothermal solution. Specifically, we report a series of new rubidium and cesium thorium fluorides, including the first characterized cesium compound, and correlate their structures to other known metal fluorides.

2. EXPERIMENTAL METHODS

2.1. Synthesis. All reagents were of analytical grade and used as purchased. Compounds in this study were prepared hydrothermally as follows: 0.15 g of ThF_4 (Strem Chemical, 99.9%) was combined with 0.3 mL of aqueous CsF (Alfa Aesar, 99.9%) or RbF (Aldrich, 99.8%), placed into a silver ampule, and weld-sealed. The sealed ampule was loaded into a Tuttle-seal autoclave, which was counter-pressured with additional water. The autoclave was heated at 575 °C for several days, typically generating a counter-pressure of 17 000 psi, resulting in a slight compression of the welded ampules. The specific reaction conditions for each crystallized product are detailed in Table 1. When the reaction was complete, the contents of the ampule were filtered and the products washed with deionized water to yield large colorless crystals. Powder X-ray diffraction was used to characterize the bulk solids, and single crystal X-ray diffraction was used to identify and structurally characterize new species.

2.2. X-Ray Diffraction. Powder X-ray diffraction (PXRD) data were collected using a Rigaku Ultima IV X-ray diffractometer with Cu Kα radiation (λ = 1.5418 Å). Patterns were collected from 5 to 60° in 2Θ at a scan speed of 1.0 deg/min. Single crystal X-ray intensity data were collected using a Rigaku Mercury CCD detector and an AFC-8S diffractometer equipped with a graphite monochromator that emits Mo Kα radiation (λ = 0.71073 Å). The space groups were determined from the observed systematic absences and confirmed using the MISSYM algorithm within the PLATON program suite.[32]

Data reduction including the application of Lorentz and polarization effects (Lp) and absorption corrections were performed using the CrystalClear program.[33] The structures were solved by direct methods and refined using subsequent Fourier difference techniques, by full-matrix least-squares, on F^2 using SHELXTL 6.10.[34] All atoms were refined anisotropically except where specified. Data from the single crystal structure refinements are given in Table 2. All single crystal solutions were confirmed by simulating the powder pattern from the single crystal structure determinations and comparing these to the powder patterns obtained from the bulk reaction products or those previously published.

3. RESULTS AND DISCUSSION

3.1. Descriptive Synthetic Chemistry. Reactions were investigated by differing pressure, reaction time, and ratios of A/Th (A = Cs, Rb) as a means to explore this phase space and identify any trends in compound formation. Crystals of **1** and **2** seem to most commonly form as a mixture of phases over a wide range of Cs/Th ratios and reaction conditions. Phase pure yields were not common but could be obtained from specific reaction conditions outlined in Table 1. PXRD patterns for these products are shown in the Supporting Information, Figure S1. It is interesting that formation of the $CsTh_3F_{13}$ phases is not limited to the lowest Cs/Th ratios, as one may expect on the basis of the chemical formula, with these crystals forming from even 9 M CsF solutions. Also of note is that only the shortest reaction using 1 M CsF concentrations afforded a phase-pure yield of hexagonal $CsTh_3F_{13}$, suggesting that a longer reaction time may cause conversion of **2** to **1**. Conditions 4 and 5 also support this as a mixture of the phases that is obtained in these longer experiments. DSC/TGA studies of the sample from condition 3 shows a transition from hexagonal compound **2** to orthorhombic compound **1** around 840 °C (Figure S2, Supporting Information), which was corroborated by PXRD of the sample before and after heating. DSC/TGA studies of the sample from phase-pure condition 2 do not exhibit the comparable endotherm, further supporting the idea that the hexagonal compound **2** is the less-stable phase. Though not detailed here, similar reaction conditions also yield several polymorphs of a different formulation, $CsThF_5$. This will be discussed in a future publication.[35]

A variety of rubidium thorium fluorides resulted from similar reactions (conditions 6−10) in Table 1. In these cases, the products seem to be fairly sensitive toward the Rb/Th ratio in the reaction. This sensitivity is in fact reflected in the chemical formulas of the products, with $RbTh_3F_{13}$ forming from the lowest RbF concentrations (Rb/Th ~ 0.4:1 to 0.8:1), $RbTh_2F_9$ from Rb/Th ~ 0.8:1, and $Rb_7Th_6F_{31}$ from Rb/Th above 1.6:1. It is especially interesting that while both **3** and **4** formed from 1 M RbF, compound **4** only formed as a minor product in the reaction occurring at higher pressures, suggesting that there may be pressure dependence in its formation. We also note that unlike the cesium thorium fluoride system, a hexagonal modification of $RbTh_3F_{13}$ has not been observed in this study.

Attempts using nearly the exact conditions that form the Cs analog **2** do not lead to the hexagonal rubidium thorium fluoride. Similarly, the formation of **5** is unique to the rubidium thorium fluoride system. The very short reaction time and somewhat elevated pressure of this reaction have been applied to cesium thorium fluoride experiments with no evidence of a Cs analog of **5**. Powder XRD from conditions 7 and 9 is shown

dx.doi.org/10.1021/ic2019555 | Inorg. Chem. 2011, 50, 11825−11831

Table 2. Crystallographic Data for Structures 1−5

	1	2	3	4	5
chemical formula	$F_{13}Th_3Cs$	$F_{13}Th_3Cs$	$F_{13}Th_3Rb$	F_9Th_2Rb	$F_{31}Th_6Rb_7$
fw (g/mol)	1076.03	1076.03	1028.59	720.55	2598.45
space group	$Pmc2_1$	$P6/mmm$	$Pmc2_1$	$Pnma$	$R\bar{3}$
temp/K	293 ± 2	293 ± 2	293 ± 2	293 ± 2	293 ± 2
cryst syst	orthorhombic	hexagonal	orthorhombic	orthorhombic	trigonal
a, Å	8.1830(16)	8.2607(12)	8.1805(16)	8.9101(18)	15.609(2)
b, Å	7.5780(15)	8.2607(12)	7.4378(15)	11.829(2)	15.609(2)
c, Å	8.6244(17)	8.6519(17)	8.6594(17)	7.1692(14)	10.823(2)
V, Å^3	534.81(18)	511.30(15)	526.88(18)	755.6(3)	2283.6(7)
Z	2	2	2	4	3
D_{calcd}, Mg/m^3	6.682	6.989	6.483	6.334	5.668
indices (min)	[−9, −9, −10]	[−10, −10, −10]	[−10, −9, −10]	[−11, −14, −8]	[−19, −19, −13]
(max)	[9, 8, 10]	[10, 10, 10]	[10, 9, 10]	[11, 14, 8]	[19, 19, 13]
params	89	26	89	59	70
F(000)	884	875	848	1192	3261
μ, mm^{-1}	45.119	47.193	46.982	45.824	40.508
2θ range, deg	3.58−25.01	2.85−26.34	2.49−26.31	3.32−26.44	2.41−26.03
collected reflns	4235	4870	4896	6376	7061
unique reflns	1008	250	1149	813	996
final R (obs. data),[a] R_1	0.0327	0.0393	0.0301	0.0797	0.0357
wR_2	0.0687	0.0976	0.0550	0.2327	0.0818
final R (all data), R_1	0.0379	0.0394	0.0364	0.0829	0.0461
wR_2	0.071	0.0977	0.0576	0.2370	0.0869
goodness of fit (S)	1.020	1.187	1.093	1.079	1.119
extinction coefficient	0.0078(3)	0.0018(4)	0.0064(2)	0.0069(11)	0.00085(4)
largest diff. peak	4.002	7.777	4.170	10.005	1.393
largest diff. hole	−2.120	−3.179	−2.287	−14.235	−2.834

[a] $R_1 = [\sum||F_o| - |F_c||]/\sum|F_o|$; $wR_2 = \{[\sum w[(F_o)^2 - (F_c)^2]^2]\}^{1/2}$.

in Figure S3 (Supporting Information), confirming the phase-pure yields of **3** and **5**. The presence of $RbTh_2F_9$ was not apparent from the powder pattern of condition 8; thus compound **4** must be a very minor product identified only by selection of an appropriate single crystal for structure analysis. A shift to higher 2Θ angles is observed for compound **3** in Figure S3 relative to compound **1** in Figure S1, accounting for the smaller unit cell volume of the Rb-containing isomorph.

3.2. Crystal Structures of Orthorhombic (A)Th_3F_{13} (A = Cs and Rb, 1 and 3, Respectively). Solids **1** and **3** both crystallize in the acentric orthorhombic space group $Pmc2_1$ (No. 26), confirmed by PXRD comparisons to previously reported powder patterns (for which no space group was determined) and those simulated from our own single crystal structure determinations.[4,8,12] Single crystals of suitable quality have not previously been synthesized for compound **1**; however, SXRD data for compound **3** were reported by Brunton[12] in the space group $P2_1ma$, a nonstandard but identical variation of $Pmc2_1$ (No. 26).[39] We were able to obtain a somewhat better structure solution for **3** (R = 0.0301) in this study than previously reported by Brunton (R = 0.0710). Atoms F1, F2, F5, F6, and F8 in compound **1** were refined using an ISOR restraint to prevent their principal mean square atomic displacements from being nonpositive definite. Both crystallographically unique thorium atoms are slightly distorted antiprisms with average Th−F distances of 2.385(8) and 2.381(9) for Th1 and Th2, respectively, in **1** and 2.377(12) and 2.373(9) Å for Th1 and Th2, respectively, in **3** (see Table 3). These correlate well with both the expected values predicted by Shannon[36] and the values found by Brunton.[12] This phase contains Th1, A1, F1, F2, F5, F6, and F9 atoms in special positions, with all having m symmetry.

Table 3. Selected Bond Distances (Å) with ESDs for Compounds 1 and 3[a]

compound 1		compound 3	
bond distances (Å)			
Th1−F2	2.482 (19)	Th1−F2	2.445 (16)
Th1−F3 (×2)	2.463 (12)	Th1−F3 (×2)	2.466 (9)
Th1−F7 (×2)	2.360 (12)	Th1−F7 (×2)	2.348 (9)
Th1−F8 (×2)	2.350 (12)	Th1−F8 (×2)	2.344 (9)
Th1−F9 (×2)	2.32 (2)	Th1−F9 (×2)	2.314 (18)
Th2−F1	2.384 (8)	Th2−F1	2.366 (6)
Th2−F2^{i}	2.480 (11)	Th2−F2^{i}	2.486 (9)
Th2−F3	2.348 (13)	Th2−F3	2.347 (10)
Th2−F4^{ii}	2.340 (12)	Th2−F4^{ii}	2.352 (10)
Th2−F4^{iii}	2.390(12)	Th2−F4^{iii}	2.369 (10)
Th2−F5	2.355 (8)	Th2−F5	2.346 (7)
Th2−F6	2.388 (9)	Th2−F6	2.386 (7)
Th2−F7	2.333 (13)	Th2−F7	2.319 (9)
Th2−F8^{iv}	2.408 (11)	Th2−F8^{iv}	2.382 (9)
Cs1−F1	2.835(16)	Rb1−F1	2.826 (13)
Cs1−F3 (×2)	3.005 (12)	Rb1−F3 (×2)	2.921 (9)
Cs1−F4 (×2)	3.222 (12)	Rb1−F4 (×2)	3.162 (9)
Cs1−F6	2.911 (16)	Rb1−F6	2.889 (13)
Cs1−F6	3.097 (14)	Rb1−F6	3.002 (15)
Cs1−F8 (×2)	3.315 (16)	Rb1−F8 (×2)	3.220 (9)

[a] Symmetry codes: (i) x, $-y$, $z + 1/2$. (ii) x, $-y + 1$, $z + 1/2$. (iii) x, $-y$, $z - 1/2$. (iv) x, $y - 1$, z.

The isostructural compounds consist of alternating edge-shared nine-coordinate thorium atoms that conform to both monocapped square antiprisms (Th1) and tricapped trigonal prisms (Th2).

dx.doi.org/10.1021/ic2019555 | Inorg. Chem. 2011, 50, 11825−11831

Unique Th atoms are edge-sharing through F2 and F3 and corner-sharing with separate connections through F7 and F8. Th1 is corner-sharing with itself through F9, while Th2 is corner-sharing with itself through F4 and F5 as well as edge-sharing with itself through F1 and F6. This results in a layered framework based on triangular clusters of thorium fluoride polyhedra with channels in the framework oriented along [010] that accommodate the Cs or Rb cations (see Figure 1). This accounts for the observed cell parameters where the *a* and *c* axes are nearly equivalent for both the Cs and Rb compounds, whereas the expected elongation associated with the presence of Cs in these channels is primarily apparent (albeit modestly) in the *b* axis length. We observe only a small difference in the average 9-coordinate alkali metal to fluorine bond distances (3.103 in **1** and 3.036 Å in **3**), as these appear to be largely governed by the diameter of the channels formed by the Th−F framework. It is reasonable to assume that smaller alkali cations Na^+ and K^+ would be very weakly bound in the channels of this structure type and would perhaps adopt a different structure type for an ATh_3F_{13} formulation. As such, the KTh_3F_{13} formulation has only been proposed in a hexagonal crystal system based on crystal morphology and thermal analysis data,[6] and no space group or unit cell parameters were reported.

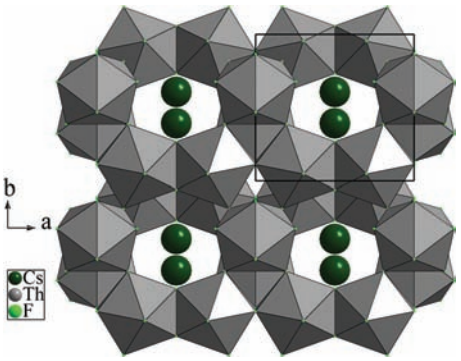

Figure 1. A view of the channel structure of **1** projected down the *c* axis.

3.3. Crystal Structures of Hexagonal $CsTh_3F_{13}$ (2). Solid **2** crystallizes in the hexagonal space group *P6/mmm* (No. 191). This hexagonal polymorph of $CsTh_3F_{13}$ has not been previously reported, and its structure is notably different from the orthorhombic phase **1**. Owing to its high symmetry, every atom save F3 sits on a special position. Cs1 and Cs2 both have *6/mmm* symmetry; Th1 has *2mm* symmetry; and F1, F2, and F4 have *m2m*, *3m*, and *mmm* symmetry, respectively. The single unique thorium atom in **2** adopts a slightly distorted monocapped square antiprismatic geometry. The thorium fluoride polyhedron is considered only slightly distorted as compared to previously reported calculations for standard monocapped square antiprisms[38] due to small variations in the Th−F bond lengths (Table 4). The apexes of these polyhedra (formed by F4) are aligned along the *c* axis and are corner-shared by neighboring Th atoms. Further connectivity of the polyhedra along the *c* axis occurs via edge-sharing of F1 atoms as well as along the *a* and *b* axes through edge-sharing of F2 and F3. Th−F bonds range from 2.301(1) Å to the apical F4 to a somewhat elongated 2.481(7) Å to F2 (see Table 4), but having an average of 2.379 Å, correlating well with the expected values predicted by Shannon.[36]

The resulting network of thorium fluoride polyhedra forms hexagonally shaped channels along the *c* direction. The boundaries of the channel are formed by alternating F1 and F3 atoms, so the channel varies in diameter from the base of each point in the hexagon, measuring 5.26(2) Å in diameter for F3 boundaries and 5.79(1) Å for F1 boundaries. Opposing Th atoms are separated by 8.261(1) Å across the channel. This leaves ample space for the cesium ions to occupy the channel (see Figure 2). Cesium(1) exhibits a six-coordinate trigonal prismatic geometry and is fairly tightly bound in this channel to F1 atoms (Cs1−F1 = 2.890(12) Å). Cesium(2) is held in place by much weaker interactions, having 12 long bonds to F3 (3.131(13) Å). The unique Cs atoms

Table 4. Selected Bond Distances (Å) with esd's for Compound 2, 4, and 5[a]

compound **2**		compound **4**		compound **5**	
		bond distances (Å)			
Th1−F1 (×2)	2.375 (6)	Th1−F1	2.367 (9)	Th1−F1	2.230 (7)
Th1−F2 (×2)	2.481 (7)	Th1−F1	2.346 (9)	Th1−F2	2.232 (6)
Th1−F3 (×4)	2.350 (6)	Th1−F2	2.338 (9)	Th1−F3	2.398 (6)
Th1−F4	2.3006 (9)	Th1−F2	2.381 (9)	Th1−F3	2.435 (6)
Cs1−F1 (×6)	2.890 (12)	Th1−F3	2.364 (10)	Th1−F4	2.357 (6)
Cs2−F3 (×12)	3.131 (13)	Th1−F3	2.417 (8)	Th1−F4	2.376 (6)
		Th1−F4	2.385 (9)	Th1−F5	2.358 (7)
		Th1−F4	2.406 (9)	Th1−F5	2.339 (7)
		Th1−F5	2.3531 (9)	Rb1−F1^{i}	2.754 (7)
		Rb1−F1 (×2)	2.772 (9)	Rb1−F1^{ii}	2.803 (7)
		Rb1−F2 (×2)	2.744 (10)	Rb1−F1	2.846 (7)
		Rb1−F3 (×2)	2.857 (12)	Rb1−F2	2.895 (7)
		Rb1−F3 (×2)	3.182 (10)	Rb1−F2	2.792 (6)
		Rb1−F4 (×2)	3.248 (10)	Rb1−F3^{iii}	2.888 (7)
				Rb1−F3^{iv}	2.901 (6)
				Rb1−F4	3.339 (7)
				Rb1−F4^{v}	3.437 (7)
				Rb1−F5^{vi}	3.252 (8)
				Rb2−F2 (×6)	2.815 (6)

[a]Symmetry codes: (i) $-x + y + 2/3, -x + 1/3, z + 1/3$; (ii) $-x + 2/3, -y + 1/3, -z + 1/3$. (iii) $x - y - 1/3, x - 2/3, -z + 1/3$. (iv) $y + 1/3, -x + y + 2/3, -z + 2/3$. (v) $x - 2/3, y - 1/3, z + 2/3$. (vi) $-y + 1/3, x - y - 1/3, z - 1/3$.

dx.doi.org/10.1021/ic2019555 | *Inorg. Chem.* 2011, 50, 11825–11831

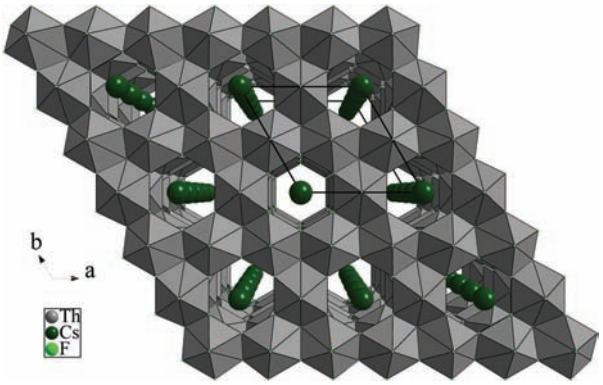

Figure 2. Perspective view of the channel structure of **2** down the *c* axis. The nine-coordinate thorium (shown as gray polyhedra) also runs infinitely in the *c* direction and forms hexagram-shaped channels where the Cs^+ (dark green) resides.

alternate along [001]. Thus, the structure is layered along [001] with a layer of thorium polyhedra followed by a layer of Cs2 atoms, then a second layer of thorium polyhedra followed by a layer of Cs1 atoms, as shown in Figure 3. Layers are also evident

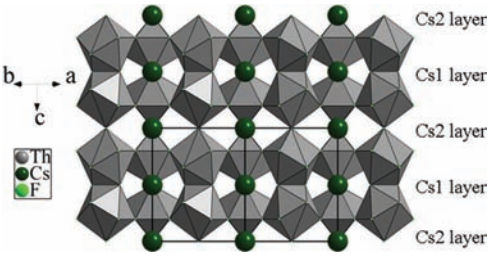

Figure 3. Layered structure of **2** viewed along the [110] direction with a single unit cell shown with black edges. The two unique cesium sites occupy different layers in an alternating fashion. This also serves as a cross-sectional view of the channel structure where only three of the six thorium polyhedra, participating in the channel construction, are currently displayed.

along [100] and [010]. Here, there is only a two-layer repeat pattern of Th polyhedra followed by a layer containing Cs1, Cs2, and Th atoms.

The structural feature distinguishing structures **1** and **2** is most obviously the shape of the channels and the direction in which they run. This is certainly dependent on the differences in thorium geometries in each, and the simpler Th−F network of **2** is reflected in its higher symmetry space group. It is interesting that, in comparing compounds **1** and **2** when two types of thorium polyhedra are present, the resulting structure is not only of lower orthorhombic symmetry but also acentric. We postulate that the larger channel diameter of **2** may factor into why an analogous hexagonal $RbTh_3F_{13}$ phase has not been obtained, as the channel present in this structure type may be too wide to support Rb at the A2 alkali metal sites.

3.4. Crystal Structure of $RbTh_2F_9$ (4). Compound **4** crystallizes in the orthorhombic space group *Pnma* (No. 62). Unfortunately, due to relatively poor crystal quality in the numerous samples tested, the best final R_1 value is somewhat high at 0.0797, and all of the atoms had to be refined using an ISOR restraint to prevent their principal mean square atomic displacements from being nonpositive definite (though Th1 still remained a nonpositive definite and was refined isotropically). However, the structure makes good chemical sense, since Brunton characterized potassium uranium fluoride, KU_2F_9, in the same space group and the atomic positions for each atom closely resemble our structure solution.[40] This new compound consists of alternating layers (along [010]) of nine-coordinate thorium atoms and rubidium atoms. The thorium atoms adopt a highly distorted tricapped trigonal prismatic geometry similar to that of Th2 in **1** and **3**. These polyhedra exhibit a preferential alignment of Th−F5 bonds along the *b* axis, which directly connect the thorium layers. The thorium fluoride polyhedron is highly distorted as compared to previously reported calculations for more typical tricapped trigonal prisms[37] due to observed variations in the Th−F bond lengths (Table 4). The Th−F bond lengths vary from 2.338(9) Å to 2.417(8) Å with an average Th−F distance of 2.373 Å.

Thorium fluoride polyhedra are edge-sharing through pairs of F1 atoms and through F2 and F3 and corner-sharing through F4 and F5 to form the layered framework. Thorium atoms connect in a zigzag fashion along [100] and [001] within their layers, as shown in Figure 4. Channels in the Th−F framework

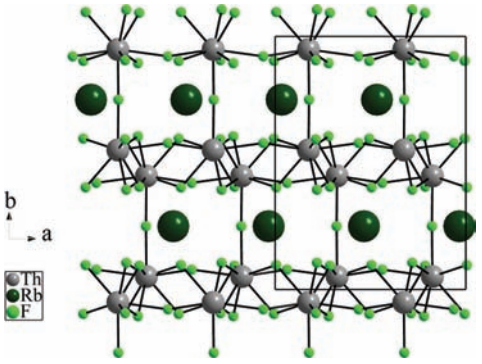

Figure 4. Compound **4** viewed down the *c* axis, showing the zigzag nature of the thorium-containing layers. Layers are connected along the *b* axis through Th1−F5−Th1 bonding as well as Rb−F interactions.

running along the [100] direction accommodate the Rb cations. These channels are shaped as hexagons elongated along the *c* axis, and Rb atoms are staggered within the channels due to the zigzag nature of the thorium fluoride framework (Figure 5). The Rb cation exhibits six typical bonds to F atoms

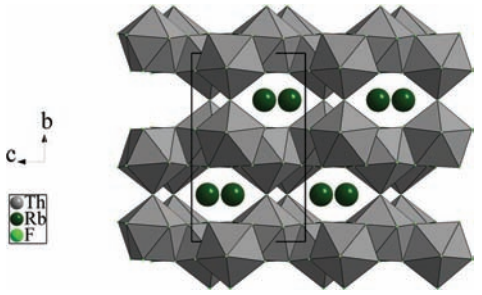

Figure 5. Channel structure in **4** viewed down the *a* axis. The nine-coordinate thorium atoms (shown as gray polyhedra) form elongated hexagon-shaped channels where the Rb^+ (dark green) can sit in a staggered formation.

(F2, F3, and F5), ranging from 2.744(10) Å to 2.857(12) Å, and two pairs of very weak interactions to each of F3 (3.182(10) Å) and F4 (3.248(10) Å) atoms. Thus, the channels here are much smaller than those in which the Rb resides in **3**.

dx.doi.org/10.1021/ic2019555 | *Inorg. Chem.* 2011, 50, 11825–11831

On the basis of the observed Rb−F bond distances in this compound (and given a comparison of the bond lengths in the compounds $K_7Th_6F_{31}$ and $Rb_7Th_6F_{31}$ discussed below), it is not surprising that powders of the previously reported KTh_2F_9 phase have been indexed in an orthorhombic crystal system (*Pnam*) with related cell parameters a = 8.85 Å, b = 7.16 Å, and c = 11.62 Å.[16] Previously reported $NaTh_2F_9$ crystallizes in an entirely different structure type (s.g. $I\bar{4}2m$).[19] However, the single crystal structure determination of KU_2F_9[40] shows that it is similar to our structure. In the single crystal structure determination of the present study, only two atoms, Rb1 and F5, sit on special positions, and both have *m* symmetry.

3.5. Crystal Structure of $Rb_7Th_6F_{31}$ (5). Compound **5** crystallizes in the trigonal space group $R\bar{3}$ (No. 148); PXRD data of the bulk sample and a simulated powder pattern from the single crystal structure in the present study are both identical to a previously reported powder pattern for **5**, for which no single crystal structure was reported.[7] Several isostructural analogs of this compound have previously been reported, including $Na_7Th_6F_{31}$ as a powder[10] and $K_7Th_6F_{31}$[13] and $Na_7Zr_6F_{31}$[37] as single crystals. We note that for this compound Rb2 sits on a $\bar{3}$ symmetry site, and the other atom in a special position, F6, happens to sit on a 3-fold rotation symmetry site.

$Rb_7Th_6F_{31}$ consists of clusters of eight-coordinate thorium atoms in a pseudosquare antiprismatic geometry and six- and seven-coordinate Rb atoms. Thorium polyhedra are edge-sharing with one another through F3 pairs and corner-sharing through F4 and F5. Thorium polyhedra are edge-sharing with seven-coordinate Rb1 polyhedra through F3 and F2 as well as F1 and F2, with additional corner-sharing through F3. Thorium(1) is only corner-sharing with six-coordinate Rb2 through F2 in this structure. Rb2 is sandwiched between Rb1 atoms by edge-sharing of F2 atoms, isolating Rb2 from itself. The resulting framework forms a cage-like structure where F6 sits in the cages with very long interactions to Th1 (2.618(5) Å) and Rb2 (3.698(5) Å). Fluorine(6) "rattles" significantly in this cage, resulting in especially large thermal parameters. This phenomenon was also observed in the potassium analog of this compound.[13] This structure type differs slightly from the others in this study in that channels are formed by a Th−F−Rb−F network, where the alkali metal not only resides in the channel (along with the F6 atom) but also contributes to determining the size of that channel (Rb1 participates in the network and Rb2 sits in the channel).

This structure type enjoys an added aspect of flexibility that could also account for the variety of different chemical formulas that accommodate this structure type. We observe Rb−F bond distances of 2.815(6) Å for Rb2 (within the channel) and an average of 2.840 Å for the nearest seven fluorines to Rb1. On the basis of ref 13, the K−F bond distances are 2.736 Å for K2 and an average of 2.698 Å for K1. In addition to the flexibility afforded by having the alkali metal as a component of the channel-forming network, adjustments in the size of the tetravalent ion (such as Zr^{4+} in $Na_7Zr_6F_{31}$) can be useful in creating channels of other sizes for alkali ions.[37] However, we have not yet observed an alkali thorium fluoride structure type flexible enough to accommodate K, Rb, and Cs when the channels are formed by only thorium fluoride bonding.

4. CONCLUSIONS

We found that hydrothermal synthesis of cesium and rubidium thorium fluorides using ThF_4 and CsF or RbF yielded a wide variety of products, including the first fully characterized cesium thorium fluorides, two new rubidium thorium fluorides, and several other previously reported rubidium thorium fluorides (Figure 6). Many of the formulations reported earlier were not

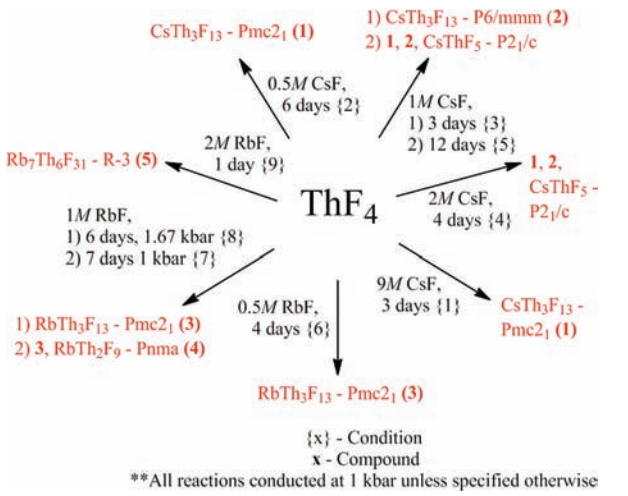

Figure 6. Specific reaction conditions for the syntheses of the title solids.

previously characterized by single crystal diffraction due to the lack of suitably high quality crystals. Some of the compounds reported herein can be prepared as phase-pure materials, opening the door for future study. Many of the compounds grow in a variety of polymorphs, indicating the richness of this phase space. The identity of the species seems to be primarily dependent on the concentration of the alkali fluoride mineralizer used in their syntheses. The resulting structures exhibit Th−F frameworks that form distinct channels in which the alkali cations reside. Given the more rigid nature of the Th−F bond (compared to Cs−F or Rb−F), the results of the present study suggest there may be some value to using the size of these channels as a predictive measure as to which other alkali thorium fluorides may crystallize in a particular structure type. Especially interesting is that we have not yet identified an alkali thorium fluoride that is isostructural for all three K, Rb, and Cs phases. For other alkali thorium fluorides where multiple compounds are reported in the literature with the same formulation, the structures of the entire series are not sufficiently characterized. The facile growth of these stable alkali thorium fluorides is an encouraging sign and may be useful if thorium is to be developed as a safe alternative nuclear fuel source in the future.

■ ASSOCIATED CONTENT

Ⓢ Supporting Information

Listings of CIF files for **1**−**5**, DSC of a sample of condition 3 (Supporting Figure 2), and comparative PXRD data (Supporting Figures 1 and 3). This material is available free of charge via the Internet at http://pubs.acs.org.

■ AUTHOR INFORMATION

Corresponding Author

*E-mail: kjoseph@clemson.edu.

■ ACKNOWLEDGMENTS

The authors thank J. David Musgraves for conducting the necessary DSC studies and the National Science Foundation (Grant #DMR-0907395) for financial support.

■ REFERENCES

(1) Brunton, G. D.; Insley, H.; McVay, T. N.; Thoma, R. E. *Crystallographic Data for Some Metal Fluorides, Chlorides, and Oxides*; ORNL-3761; U.S. Government Printing Office: Washington, DC, 1965.
(2) (a) Jacoby, M. *Chem. Eng. News* **2009**, *87* (46), 44−46. (b) Svoboda, E. The Truth About Thorium and Nuclear Power. *Popular Mechanics*, October 20, **2010**. (c) Kazimi, M. Thorium Fuel for Nuclear Energy. *American Scientist*; **2003**, *91* (5), 408−412. (d) Bagla, P. *Science* **2005**, *309*, 1174−1175. (e) Biello, D. China Syndrome: Going Nuclear to Cut Down on Coal Burning. *Scientific American*, March 28, **2011**.
(3) Mann, M.; Thompson, D.; Serivalsatit, K.; Tritt, T. M.; Ballato, J.; Kolis, J. *Cryst. Growth Des.* **2010**, *10*, 2146−2151.
(4) Thoma, R. E.; Carlton, T. S. *J. Inorg. Nucl. Chem.* **1961**, *17*, 88−95.
(5) Harris, L. A.; White, G. D.; Thoma, R. E. *J. Phys. Chem.* **1959**, *63*, 1974−1975.
(6) Asker, W. J.; Segnit, E. R.; Wylie, A. W. *J. Chem. Soc.* **1952**, 4470−4479.
(7) Thoma, R. E. *Phase Diagrams of Nuclear Reactor Materials*; ORNL-2548; U.S. Government Printing Office: Washington, DC, 1959.
(8) Derganov, E. P.; Bergman, A. G. *Dokl. Akad. Nauk* **1948**, *60*, 391.
(9) Thoma, R. E.; Insley, H.; Landau, B. S.; Friedman, H. A.; Grimes, W. R. *J. Phys. Chem.* **1959**, *63*, 1266−1274.
(10) Thoma, R. E.; Insley, H.; Herbert, G. M.; Friedman, H. A.; Weaver, C. F. *J. Am. Ceram. Soc.* **1963**, *46*, 37−42.
(11) Harris, L. A. *Acta Crystallogr.* **1960**, *13*, 502.
(12) Brunton, G. D. *Acta Crystallogr., Sect. B* **1971**, *B27*, 1823−1826.
(13) Brunton, G. D. *Acta Crystallogr., Sect. B* **1971**, *B27*, 2290−2292.
(14) Ryan, R. R.; Penneman, R. A. *Acta Crystallogr,. Sect. B* **1971**, *B27*, 829−833.
(15) Brunton, G. D. *Acta Crystallogr., Sect. B* **1972**, *B28*, 144−147.
(16) Zachariasen, W. H. *J. Am. Chem. Soc.* **1948**, *70*, 2147−2151.
(17) Grzechnik, A.; Fechtelkord, M.; Morgenroth, W.; Posse, J. M.; Friese, K. *J. Phys.: Condens. Matter* **2007**, *19*, 266219.
(18) Zachariasen, W. H. *Acta Crystallogr.* **1949**, *2*, 390−393.
(19) Grzechnik, A.; Morgenroth, W.; Friese, K. *J. Solid State Chem.* **2008**, *181*, 971−975.
(20) Cousson, A.; Pagès, M. *Acta Crystallogr., Sect. B* **1978**, *B34*, 1776−1778.
(21) Pulcinelli, S. H.; de Almeida Santos, R. H.; Senegas, J. *J. Fluorine Chem.* **1989**, *42*, 41−50.
(22) Laligant, Y.; LeBail, A.; Avignant, D.; Cousseins, J. C.; Ferey, G. *J. Solid State Chem.* **1989**, *80*, 206−212.
(23) Laligant, Y.; Ferey, G.; El Ghozzi, M.; Avignant, D. *Eur. J. Solid State Inorg. Chem.* **1992**, *29*, 497−504.
(24) Ryan, R. R.; Penneman, R. A.; Rosenzweig, A. *Acta Crystallogr., Sect. B* **1969**, *B25*, 1958−1962.
(25) Penneman, R. A.; Ryan, R. R.; Kressin, I. K. *Acta Crystallogr., Sect. B* **1971**, *B27*, 2279−2283.
(26) Gaumet, V.; El Ghozzi, M.; Avignant, D. *Eur. J. Solid State Inorg. Chem.* **1995**, *32*, 893−905.
(27) Brunton, G. D. *Acta Crystallogr., Sect. B* **1970**, *B26*, 1185−1187.
(28) Brunton, G. D.; Sears, D. R. *Acta Crystallogr., Sect. B* **1969**, *B25*, 2519−2527.
(29) Zachariasen, W. H. *Acta Crystallogr.* **1948**, *1*, 265−269.
(30) Zachariasen, W. H. *Acta Crystallogr.* **1949**, *2*, 388−391.
(31) Stritzinger, J.; McMillen, C. D.; Kolis, J. *J. Chem. Crystallogr.* Submitted.
(32) Spek, A. L. *PLATON*; Utrecht University: Utrecht, The Netherlands, 2003.
(33) *CrystalClear* ; Rigaku/MSC: The Woodlands, TX, 1999.
(34) Sheldrick, G. M. *SHELXTL*, version 6.1; Bruker Analytical X-Ray Systems Inc.: Madison, WI, 2000.
(35) Underwood, C. C.; Mann, M.; McMillen, C. D.; Musgraves, J. D.; Kolis, J. W. *Solid State Sci.* Submitted.
(36) Shannon, R. D. *Acta Crystallogr.* **1976**, *A32*, 751.
(37) Burns, J. H.; Ellison, R. D.; Levy, H. A. *Acta Crystallogr., Sect. B* **1968**, *B24*, 230−237.
(38) Robertson, B. E. *Inorg. Chem.* **1977**, *16*, 2735−2742.
(39) *International Tables for Crystallography*; Hahn, T. Ed.; Kluwer Publishers: Dordrecht, The Netherlands, 1996; Vol *1*.
(40) Brunton, G. *Acta Crystallogr., Sect. B* **1969**, *B25*, 1919−1921.